[4]For the 23.9-keV transition in ^{119}Sn, see J. P. Bocquet *et al.*, Phys. Rev. Letters 17, 809 (1966), and G. T. Emery and M. L. Perlman, Phys. Rev. 131, 3885 (1970); for the 8.4-keV transition in ^{169}Tm, T. A. Carlson, P. Erman, and K. Fransson, Nucl. Phys. A111, 371 (1968); for the 14.4-keV transition in ^{57}Fe, F. T. Porter and M. S. Freedman, Phys. Rev. C 3, 2285 (1971). See also M. L. Perlman and G. T. Emery, Brookhaven National Laboratory Report No. BNL-13921 (unpublished), where the unpublished data by R. Martin *et al.* for the 35.5-keV transition in ^{125}Te are cited.

[5]M. Fujioka and K. Hisatake, Phys. Letters 40B, 99 (1972).

[6]M. Fujioka, Nucl. Phys. A153, 339 (1970).

[7]N. Benczer-Koller and R. H. Herber, in *Chemical Applications of Mössbauer Spectroscopy*, edited by V. I. Goldanskii and R. H. Herber (Academic, New York, 1968), p. 122.

[8]H. C. Pauli, The Niels Bohr Institute Report, University of Copenhagen, 1968 (unpublished).

[9]F. Herman and S. Skillman, *Atomic Structure Calculations* (Prentice-Hall, Englewood Cliffs, N.J., 1963).

[10]R. Ingalls, Phys. Rev. 155, 157 (1967).

[11]E. M. Anderson, M. A. Listengarten, and M. A. Khanonkind, Izv. Akad. Nauk Ser. Fiz. 34, 850 (1970); I. M. Band, L. A. Sliv, and M. B. Trzhakovskaya, Nucl. Phys. A156, 170 (1970). It is very important to note that the proportionality between the conversion probability and the electron density at the nucleus does not imply that conversion occurs just around the nuclear region. As Band *et al.* have shown, the region of conversion formation is much smaller than the atomic dimension but at the same time much larger than the nuclear dimension. The proportionality is a result of the definite shape of the radial function in this region, which depends only on the strong unscreened Coulomb, centrifugal, and spin-orbit potentials, or on the finite size of the nucleus, and is almost independent of the principal quantum number, the shape of the screening function, etc.

[12]S. Wakoh and J. Yamashita, J. Phys. Soc. Japan 25, 1272 (1968).

[13]K. J. Duff and T. P. Das, Phys. Rev. B 3, 2294 (1971).

PHYSICAL REVIEW B VOLUME 7, NUMBER 1 1 JANUARY 1973

Magnetic Anisotropy and Conduction-Electron Exchange Polarization in Ferromagnetic (Rare-Earth)Al_2 Compounds

N. Kaplan* and E. Dormann
II Physikalisches Institut, Technische Hochschule, Darmstadt, Germany

and

K. H. J. Buschow
Philips Research Laboratories, Eindhoven, The Netherlands

and

D. Lebenbaum
The Racah Institute of Physics, The Hebrew University, Jerusalem, Israel

(Received 28 July 1972)

^{27}Al NMR in ferromagnetic RAl_2 (R = Pr, Nd, Sm, Gd, Tb, Dy, Ho) has been studied. The easy direction of magnetization has been observed experimentally for the first time and a theoretical calculation, in accord with the observation, has been developed. The s-f exchange parameters have been examined and in addition to the isotropic exchange parameter Γ_{sf}, the existence of a small but significant anisotropic s-f exchange term is verified experimentally for the first time. The accurately determined (±1%) isotropic exchange parameters are compared with presently available theoretical predictions.

I. INTRODUCTION

Magnetic properties of the RAl_2 (R = rare earth) intermetallic compounds[1] were studied extensively during the last ten years. Magnetization[2] and neutron-diffraction[3,4] measurements verified that the compounds order magnetically below a transition temperature and form, in most cases, ferromagnets. Studies of magnetic transition temperature,[2-5] paramagnetic ^{27}Al Knight shifts,[6-10] and more recently, susceptibility[11] and resistivity[5,12] have been conducted in attempts to illuminate various aspects of the interactions between the presumably localized R spins and the electronic conduction band. Several groups[9,13-16] have studied the ^{27}Al hyperfine interactions in the *ferromagnetic* phase of $GdAl_2$, and it was demonstrated[14(a),16] that a slightly modified Ruderman–Kittel–Kasuya–Yosida (RKKY) model can adequately account for the relevant experimental observations.

The present report describes an extension of the ^{27}Al hyperfine field study to the ferromagnetic phases of compounds with non-S-state ions, ranging from $PrAl_2$ up to $HoAl_2$, with the exception of $EuAl_2$. The investigation was aimed at studying two phenomena: (a) the magnetic anisotropy and its variation across the group and (b) the variation of the s-f exchange across the series. Very

little has been reported previously[2] concerning the magnetic anisotropy of these compounds. In the present study the easy direction of magnetization for all the compounds has been determined for the first time, and a unified model is developed which can account—with the exception of $HoAl_2$—for the experimental results and predict the easy direction of magnetization all across the RAl_2 series.

Concerning s-f exchange polarization of conduction electrons, one would expect the RAl_2 to be nearly ideal for such study: The crystals are cubic, the R sites are well separated, [1] minimizing direct R-R exchange, the Al sites where the s-f polarization is sampled carry no localized magnetic moment, [3,4] and finally, all of the RAl_2 form an isostructural family with lattice-constant variation of less than 3% across the system. However, most of the pioneer investigations, including those concerned specifically with the variation of the effective exchange parameter Γ_{sf} across the system, [5–8] were based on the inherently inaccurate technique[10(a),10(b)] of deriving Γ_{sf} from the paramagnetic ^{27}Al Knight shifts. Subsequent reexamination of the Knight shifts, [9,10(a)] while still not accurate, indicates a different Γ_{sf} behavior, more in accord with exchange-parameter values derived from measurements of the paramagnetic Curie temperature Θ_C and of resistivity, [11,12] The latter two techniques, however, do not provide Γ_{sf} in a direct manner. Γ values derived from[5] Θ_C could include direct exchange contribution of unknown size and sign whose variation across the system does not have to be even proportional to Γ_{sf}. On the other hand, Γ_{sf} values derived from resistivity depend on knowing *a priori* the effective-mass values of the conduction electrons, which have not yet been measured independently in any of the RAl_2.

With the advent of band-structure calculations in rare-earth crystals, [17(a),17(b)] more realistic model calculations have become possible. A general theory concerned with the variation of the s-f exchange in rare earths has been developed by Watson, Koide, Peter, and Freeman[17(c)] (WKPF) and it was felt that more accurate determination of the pertinent s-f exchange parameters is desirable. The present study provides, within the framework of the RKKY model, highly accurate exchange parameters and indicates the existence small but significant anisotropic s-f exchange.

The report is organized as follows: The experimental part which consisted of obtaining the ^{27}Al NMR absorption in ferromagnetic domains of RAl_2 is described in Sec. II. The derivations of the easy direction of magnetization and of the ^{27}Al hyperfine fields are described in Sec. III. A model calculation of the magnetic anisotropy is given in Sec. IV and the behavior of the exchange interaction, as derived from the ^{27}Al hyperfine fields, is discussed in Sec. V.

II. EXPERIMENTAL PROCEDURES AND RESULTS

The samples RAl_2 were prepared by arc melting rare-earth elements and aluminium of 99.9% and 99.99% purity, respectively. X-ray diffraction showed the as cast samples to be free of any second phases. It was found for some of the samples that annealing (about 45 h at 900 °C) did not change the NMR spectra significantly. The present investigation was therefore performed with as cast samples which were then pulverized to ensure adequate rf penetration.

For $GdAl_2$, several samples were prepared with varied exposures to hammering during the milling process and with particle size ranging between $\sim 100\ \mu$ to smaller than $\sim 30\ \mu$. Only one sample for each of the other RAl_2 was prepared, all with a relatively long time in the milling machine, with particle sizes $< 50\ \mu$. The powder samples were then usually immersed in silicon oil in glass vials and placed inside the spectrometer coil with both coil and vial immersed in the He bath.

The ^{27}Al NMR line profiles were obtained with a "Bruker" variable-frequency spectrometer. The procedure consisted of measuring, under zero external field, the spin-echo amplitude as a function of frequency at 200-kHz intervals. The value of H_1 was optimized at some frequency where echos could be observed, and then kept usually constant throughout the frequency range. In all cases, a combination of rather large H_1 (10–50 G) and narrow (~ 1–$3\ \mu$sec) pulse widths was required to optimize the spin-echo amplitude, indicating that most of the signals came from nuclei in domains. The over-all gain and sensitivity of the spectrometer throughout the frequency range was calibrated by a sample of protons. The spin-echo amplitude, extrapolated to $\tau = 0$ to correct for T_2 variation across the line profile and corrected by the gain calibration function, was plotted for each sample as a function of frequency. The results for $T = 4.2$ °K are shown in Fig. 1. The absorption profiles for various $GdAl_2$ samples—prepared as discussed above—are plotted in Fig. 2. Frequency shifts of prominent peaks in the line profile could be detected upon application of external magnetic field. As shown in line 3 of Table I, positive shifts were observed for $R = Pr$, Nd, and Sm and negative shifts for Gd, Tb, Dy, and Ho. The approximate zero-field relaxation times, T_1 and T_2, observed for some samples are also listed (lines 3 and 4 of Table II) although no discussion of relaxation is intended in the present paper. In several samples, notably in $GdAl_2$, $HoAl_2$, $TbAl_2$, and $NdAl_2$ echo-amplitude oscillation was observed as a function of the separation τ between the two rf pulses. A pre-

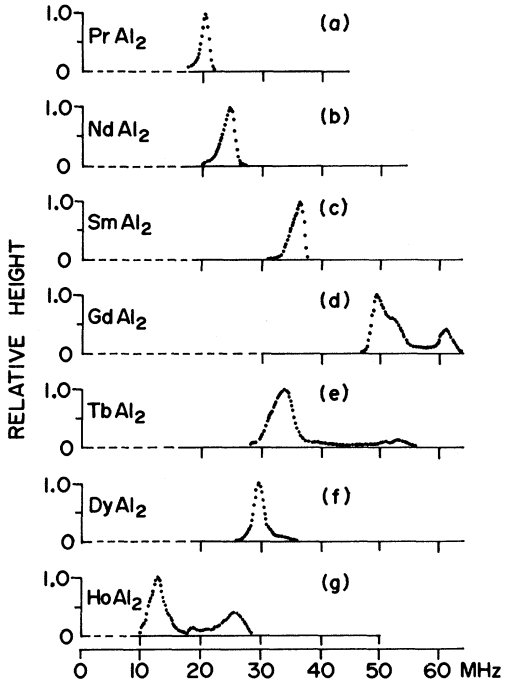

FIG. 1. Calibrated ^{27}Al NMR profiles in ferromagnetic RAl_2.

liminary study of the oscillation in $GdAl_2$ was reported previously,[14] and while a detailed report of the phenomenon—which is attributed to static electric quadrupole interaction—will be given elsewhere, the approximate fundamental oscillation frequencies, $f(\tau)$, are listed (line 2 of Table II) for the sake of completeness.

III. DERIVATION OF MAGNETIZATION DIRECTION AND ^{27}Al HYPERFINE FIELDS

The $GdAl_2$ profiles [Figs. 1(d) and 2] have been identified with ^{27}Al NMR previously.[9,14] For the other compounds, measurements in the ferromagnetic phase have not yet been reported and it is necessary to establish the identity of the profiles [Figs. 1(a)–1(c) and 1(e)–1(g)]. For non-S-state R ions, the NMR absorption of R nuclei is expected usually at the 1-GHz frequency range because of large orbital effective fields. While large single-ion quadrupole interaction could lead to absorption also in the 50–100-MHz range, no such transitions have so far been observed.[18] Moreover, there is experimental evidence that the present profiles are not due to R nuclei: (a) T_2 values expected for R nuclei at 4.2 °K are in the 10^{-5}-sec range,[18] whereas T_2 values observed presently (Table II, line 3) are in the 10^{-4}–10^{-3}-sec range; and (b) the shift of the profiles, upon application of external field, reverses sign (Table I, line 3) when crossing from

TABLE I. Hyperfine and exchange parameters in ferromagnetic RAl_2.

	$PrAl_2$	$NdAl_2$	$SmAl_2$	$GdAl_2$	$TbAl_2$	$DyAl_2$	$HoAl_2$	$HoAl_2$
$\vec{M}$ direction[a]	[100]	[100]	[111]	[111]	[111]	[100]	[111]	[110][b]
ν (MHz)	20.4 ± 0.1	24.7 ± 0.1	a: 35.1 ± 0.2 b: 36.4 ± 0.1	a: 61.15 ± .05 b: 49.45 ± .05	a: 53.0 ± 0.4 b: 34.1 ± 0.1	29.8 ± 0.1	a: 25.6 ± 0.1 b: 12.8 ± 0.1	a: 25.6 ± 0.1 b: 12.8 ± 0.1
Sign of $\frac{d\nu}{dH_{ext}}$	+	+	+	–	–	–	–	–
H_d^{cal} (kG)	2.19	2.26	0.71 (a site)	7.10 (a site)	9.26 (a site)	7.34	10.49 (a site)	9.08 (a site)
H_d^{expt} (kG)			0.87 ± 0.2 (a site)	8.03 ± 0.1 (a site)	13.26 ± 0.4 (a site)		9.30 ± 0.2	8.96 ± 0.14
$\alpha = H_d^{expt}/H_d^{cal}$			1.23 ± 0.25	1.13 ± 0.02	1.43 ± 0.05		0.89 ± 0.02	0.986 ± 0.01
$H_d^{enhanced} = 1.3H_d^{cal}$	2.85	2.93				9.54		
H_{hf} (kG)[c]	+18.17 ± 0.1	+22.08 ± 0.1	+32.51 ± 0.2	−47.09 ± 0.1	−34.51 ± 0.4	−25.11 ± 0.1	−13.77 ± 0.2	−16.71 ± 0.1
Γ_{sf}^{red}	1.688 ± 0.009	1.337 ± 0.006	1.353 ± 0.008	1.0 ± 0.002	0.885 ± 0.101	0.747 ± 0.003	0.512 ± 0.007	0.621 ± 0.004

[a] Directions derived from the experimental profile (Sec. III).
[b] [110] assignment is not in accord with experiment (see text for details).
[c] For [100] domains, $H_d^{enhanced}$ was used to derive H_{hf}.

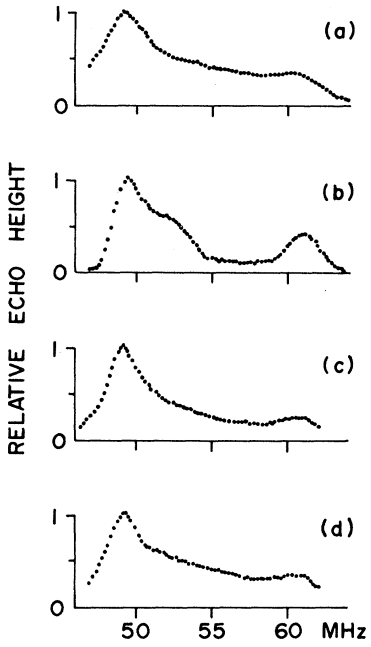

FIG. 2. Effects of strain and particle size on ^{27}Al NMR in ferromagnetic $GdAl_2$. (a) $<50\ \mu$, milled for a relatively long time; (b) $\sim 60\ \mu$, only briefly milled; (c) 90–120 μ. Particle sizes larger than rf skin depth, $\lambda \sim 1/\sqrt{\nu}$, and thus reduced absorption at higher frequency; (d) same as (a), but annealed following the milling process.

ions with $J = L - S$ (up to $SmAl_2$) to ions with $J = L + S$ ($GdAl_2$ and up), and such sign reversal is not expected for R atoms in which H_{eff} is mostly of orbital origin. Finally, we note that ^{27}Al saturation effective fields derived from Knight shifts[6,10(a)] fall within $\pm 30\%$[19] of the effective fields derived in the present study. We therefore conclude that all of the absorption profiles shown in Fig. 1 are to be associated with effective field H_{eff} acting on ^{27}Al nuclei.

A simple physical model can account phenomenologically for the profiles of Fig. 1. In this model the total effective field is written as the vector sum of two contributions

$$\vec{H}_{eff} = \vec{H}_{hf} + \vec{H}_d \ . \tag{1}$$

The first term $\vec{H}_{hf}$ arises from the contact interaction between s-f exchange-polarized conduction electrons and the ^{27}Al nucleus, and for a parabolic conduction band, one can express $\vec{H}_{hf}$ in terms of the RKKY model[5] as

$$\vec{H}_{hf} = \frac{9\pi Z^2 A^{27}(0)}{4E_f g_I^{27} \mu_I} \langle \vec{S} \rangle \Gamma_{sf} \sum_n F(2k_f R_n) \ . \tag{2}$$

For rare-earth crystals with $\vec{J}$ as the good quantum number,[5(b)] (2) can be rewritten in the form

$$\vec{H}_{hf} = (\text{const}) \frac{A^{27}(0)}{E_f} \Gamma_{sf} (g_J - 1) \langle \vec{J} \rangle \ . \tag{3}$$

From (3) it is evident that $\vec{H}_{hf}$ is isotropic, in the sense that $|\vec{H}_{hf}|$ is independent of the *direction* of $\vec{M}$ and is pointing parallel or antiparallel to $\vec{M}$, depending on the signs of Γ_{sf} and $(g_J - 1)$. The second term in (1), $\vec{H}_d$, represents the magnetic field induced at the Al site by the localized magnetic moments residing at the R sites. Using the Lorentz technique, we can actually calculate $\vec{H}_d$. For point dipoles $\vec{\mu}$ in a domain with magnetization direction $\vec{n}$,

$$\vec{H}_d = \frac{\mu}{a^3} \left[\sum_i \left(\frac{3(\vec{n} \cdot \vec{r}_i)\vec{r}_i}{r_i^2} - \vec{n} \right) \right] + \vec{H}_c \ , \tag{4}$$

where a is the lattice constant and $\vec{r}_i$ is the vector distance from an R atom at site i to the Al site, measured in units of a. The summation is over R atoms in a sphere, around the Al site, large enough to ensure proper convergence, and $\vec{H}_c$ is a correction term for nonspherical domains, given by

$$\vec{H}_c = (\tfrac{4}{3}\pi - \tilde{D})\vec{M} \ , \tag{5}$$

where $\tilde{D}$ is the demagnetization tensor whose elements are bounded, $0 < D_{mn} < 4\pi$. H_c can assume positive and negative values and for more or less "regular" random shape domains, $|H_c| \lesssim \frac{4}{3}\pi M$. Until otherwise stated, we shall assume spherical

TABLE II. Decay times and echo-modulation frequency in ferromagnetic RAl_2 in zero external field.

	$PrAl_2$	$NdAl_2$	$SmAl_2$	$GdAl_2$	$TbAl_2$	$DyAl_2$	$HoAl_2$
Echo modulation observed at 4.2 °K	no	very weak ~5%	(?) beating, weak	yes	*a*: ? *b*: yes	no	yes(~50%) (for *a*)
Frequency, $f(\tau)$ (KHz)	...	334±25	*b*: ~330 (?)	*a*: 520±50 *b*: 240±20	*a*: ~460 *b*: 286±25	...	*a*: 510±45 *b*: 260±10
T_1	~100 msec	~10 msec	~1 sec	~20 msec	<10 msec	$\gtrsim$ 100 msec	<10 msec
T_2 (μsec)	460±150	174±25	550±100	*b*: ~500	*a*: ~30 *b*: 104±5	480±50	*a*: 86±20 *b*: 124±25

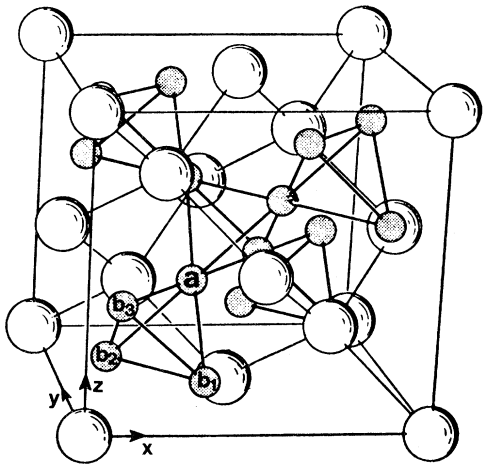

FIG. 3. The RAl_2 unit cell. Large circles represent R sites and small shaded circles represent Al sites. The coordinates of representative Al sites are a $(\frac{3}{8}, \frac{3}{8}, \frac{3}{8})$; b_1 $(\frac{3}{8}, \frac{1}{8}, \frac{1}{8})$; b_2 $(\frac{1}{8}, \frac{3}{8}, \frac{1}{8})$; b_3 $(\frac{1}{8}, \frac{1}{8}, \frac{3}{8})$.

domains, i.e., $H_c = 0$. In order to preserve maximum possible accuracy for various derived parameters, $\vec{H}_d$ values had to be calculated with $\pm 2‰$ accuracy. This was achieved by extending the summation in (4) over 100-Å radius, including approximately 2.5×10^4 R sites. Unlike $\vec{H}_{hf}$, the dipolar field as given in (4) is not isotropic. There are 16 Al sites in the RAl_2 unit cell (Fig. 3) forming four corner-sharing tetrahedra. While the point symmetry of the R sites belong to the cubic (T_d) group, the symmetry around the Al sites is much lower, belonging to a rhombohedral point group. As a result, when $\vec{M}$ is pointing in arbitrary direction, each of the four Al sites in a tetrahedron, such as sites a, b_1, b_2, and b_3 in Fig. 3, is subjected to a different H_d, and therefore different H_{eff}, value. Thus, there are in the general case four groups of magnetically inequivalent Al sites. The number of inequivalent groups is reduced when $\vec{M}$ is directed along one of the cubic symmetry axes, as can be verified either from symmetry consideration or by actually performing the summation (4). This is demonstrated in Table III, where $\vec{H}_d$ as given in (4) is calculated with $\mu = 7\mu_B$ and $a(GdAl_2) = 7.900$ Å, for [111], [110], and [100] domains. To obtain the directed angle between the vector fields in Table III, as well as for the other compounds, the direction of $\vec{H}_{hf}$, with respect to $\vec{M}$, was assumed to follow the sign of the shifts (Table I, line 3). This assumption is valid as long as the relation

$$|\vec{H}_{eff}| - |\vec{H}_d| > |\vec{H}_d| \qquad (6)$$

holds even for the maximum possible $|\vec{H}_d|$, which is indeed the case for all of the present compounds, except for the lower resonance of $HoAl_2$. Using Table III, it is concluded that for [111] magnetization, two site groups are formed, with a number ratio of 1:3. For [110] magnetization, two groups with 2:2 ratio are formed and for [100] domains, and all four sites become equivalent. For random shape [100], [111], [110] or [other] domains, the present model predicts one, two (3:1), two (2:2), or four (1:1:1:1) ^{27}Al absorption lines respectively, each broadened, or smeared out, by distribution of H_c values which are typically in the range of $\pm\frac{4}{3}\pi M$.[20]

Turning now first to the $GdAl_2$ profiles [Fig. 1(d)], it is seen that apart from some background absorption, it consists of two peaks centered around $\nu = 49.45$ MHz and $\nu = 61.15$ MHz. The half-width of each peak is of the order of 3 MHz or 3 kOe, comparable to the expected distribution of $H_c \approx \frac{4}{3}\mu M$, and the ratio of the areas under the two peaks is very nearly 3:1. In accordance with our model and Table III, we must conclude: (i) At 4.2 °K, $GdAl_2$ forms mostly [111] domains; (ii) the low-frequency peak is to be associated with (b_i) sites ($i = 1, 2, 3$) and the high one with (a) sites. With the help of Eqs. (1)–(3) and Table III, we may write

$$H_{eff}(a) = H_{hf}(a) + H_d^{cal}(a)\ , \qquad (7)$$

$$H_{eff}^2(b) = H_{hf}^2(b) + [H_d^{cal}(b)]^2 - 2H_{hf}(b)H_d^{cal}(b)\cos[\vec{H}_{hf}(b), \vec{H}_d^{cal}(b)]\ . \qquad (8)$$

The notation H_d^{cal} is used throughout to denote dipolar field calculated with $\vec{\mu} = g_J\mu_B\vec{J}$.

At this point, if we prefer to adhere to our model, (7) and (8) can be solved separately for $\vec{H}_{hf}$ after substituting experimental values, $2\pi\nu/\gamma^{27}$, for H_{eff}, and using H_d values from Table III.[21] However, a more physical approach would be to solve (7) and (8) simultaneously for H_d and H_{hf}. Such a solution is possible if we assume $H_{hf}(a) = H_{hf}(b)$

TABLE III. Dipolar field H_d^{cal} at Al sites in $GdAl_2$ (in G).

Direction of $\vec{M}$	Site[a]	$H_d(x)$ [b]	$H_d(y)$ [b]	$H_d(z)$ [b]	H_d [b]	$\cos(H_d, H_{hf})$
[111]	a	−4100	−4100	−4100	7101	1
	b_1	4100	0	0	4100	$-1/\sqrt{3}$
	b_2	0	4100	0	4100	$-1/\sqrt{3}$
	b_3	0	0	4100	4100	$-1/\sqrt{3}$
[110]	a	−2511	−2511	−5022	6151	$1/\sqrt{3}$
	b_1	2511	2511	0	3554	−1
	b_2	2511	2511	0	3554	−1
	b_3	−2511	−2511	5022	6151	$1/\sqrt{3}$
[100]	a	0	−3550	−3550	5021	0
	b_1	0	3550	3550	5021	0
	b_2	0	−3550	3550	5021	0
	b_3	0	3550	−3550	5021	0

[a]The site coordinates are: $a(\frac{3}{8}, \frac{3}{8}, \frac{3}{8})$; $b_1(\frac{3}{8}, \frac{1}{8}, \frac{1}{8})$; $b_2(\frac{1}{8}, \frac{3}{8}, \frac{1}{8})$: $b_3(\frac{1}{8}, \frac{1}{8}, \frac{3}{8})$.

[b]Computed with $a = 7.900$ Å, $J = \frac{7}{2}$, from Eq. (4). For other a and J values, multiply by $(7.9\times10^{-8}/a)^3\frac{1}{7}g_J J$.

$= H_{hf}$, because there is a simple relation between the dipole field at (a) and (b), independent of the size of $\vec{\mu}$ and given by

$$H_d(a) = \sqrt{3}\, H_d(b) \ . \tag{9}$$

In following this procedure, the assumption of completely isotropic s-f exchange-polarized contact term and a strictly point dipole term are abandoned: $\vec{H}_{hf}$ will represent the isotropic part of a more general s-f exchange contact term and the dipolar term, denoted $\vec{H}_d^{expt}$, will represent the combined contribution from point dipoles at R sites and the anisotropic part of the total s-f exchange contact term.[22] This "modified model", in which a non-negligible anisotropy of the s-f exchange interaction would manifest itself by H_d^{expt} being significantly larger than H_d^{cal},[23] is adopted for analysis purposes throughout the present investigation. The results for H_{hf} and H_d^{expt}, as applied for $GdAl_2$, are listed in the Gd column of Table I. The overall accuracy of H_{hf} is close to $\pm 2\%$ ($\pm 5\%$ for most other compounds) and H_d^{expt} is "enhanced" by about 13% over the calculated H_d^{cal} value, i.e., $\alpha = H_d^{expt}/H_d^{cal} = 1.13$. Before turning to the other compounds a final note concerning the background absorption in $GdAl_2$. As seen in Fig. 2, the character of the background depends on sample preparation techniques. A more detailed discussion has been given in Ref. 16, where it is concluded that background may be attributed to strained domains in which fluctuation of the direction of $\vec{M}$ is to be expected. The effect of such fluctuating $\vec{M}$ on absorption profiles is more pronounced for [111] domains than, say, [100] domains, because in the latter the anisotropic field H_d adds up only in quadrature to H_{hf}.

The absorption profiles of the other compounds can be analyzed in much the same way as the $GdAl_2$ profile, and in the next subsection we shall merely point out special features pertaining to the individual cases.

$TbAl_2$. In view of the remark concerning background absorption, and since, except for $GdAl_2$, all compounds were subjected to long milling during the preparation process (see Sec. II) the poor resolution of the $TbAl_2$ spectrum [Fig. 1(e)] is to be expected. Actually, the general shape of the $TbAl_2$ profile is quite similar to the profiles of strained $GdAl_2$ samples (Fig. 2). Analyzing the spectrum exactly in the same way as for $GdAl_2$, the poor resolution is reflected by the $\sim \times 5$ larger probable errors quoted for $\nu(a)$, H_d^{expt} and H_{hf} (Table I). It is concluded that $TbAl_2$ forms mostly [111] domains, and in spite of the quoted errors, the existence of a largely enhanced H_d ($\alpha = 1.43$) is evident.

$SmAl_2$. Two points to be noted. (i) H_d^{cal} for this compound is an order of magnitude smaller than in all other compounds (see Table I, line 4) and is of the order of magnitude of the typical spread, $\sim \frac{4}{3}\pi M$, arising from the distribution of the demagnetization field H_c [expression (5)]. (ii) As can be derived from the positive sign of $\partial H/\partial \nu$, the direction of $\vec{H}_{hf}$ in $SmAl_2$ is along $\vec{M}$, compared to the antiparallel direction in $GdAl_2$ and $TbAl_2$, and therefore in the present case $\nu(a) < \nu(b)$. Indeed, in accordance with the above remarks, the unresolved asymmetric line shape shown in Fig. 1(c) can be reconstructed (Fig. 4) by adding up two closely spaced line shapes of unequal intensity, with the smaller one at lower frequency, each with a half-width of $\sim \frac{4}{3}\pi M$ and a small background intensity. It is thus concluded that $SmAl_2$ forms [111] domains. The smallness of H_d results in a large fractional error bracket on H_d^{expt}, with $\alpha = 1.25 \pm 0.25$, but for the very same reason, $\vec{H}_{hf}$ could be determined with an accuracy of $\pm 0.6\%$ in spite of the unresolved profile. As a matter of fact, even if for some reason the [111] domain assignment is erroneous (e.g., supposing the profile represents unsplit sites from [100] domains or equal intensity doublet from [110] domains and the observed asymmetry is spurious...), the value of H_{hf} will remain essentially unchanged.

It should be pointed out that an "anomalous" negative ^{27}Al Knight shift (KS) has been observed in the *paramagnetic* phase of $SmAl_2$,[10(c)] in apparent disagreement with the positive $\partial\nu/\partial H$ reported presently for *ferromagnetic* $SmAl_2$ at 4.2 °K. The negative KS indicates a complete breakdown of the relation $\vec{S} \to (g_J - 1)\vec{J}$, used in the transformation from Eq. (2) to Eq. (3), for the paramagnetic phase, possibly through the interplay between crystal field and higher Sm^{3+} excited levels occurring at the elevated temperature range in which the KS study has been conducted.

$PrAl_2$. From the single line spectrum [Fig. 1(a)] it is concluded immediately that $PrAl_2$ forms [100] domains. For the [100] configuration there are no longer two independent relations, such as (7) and (8) connecting H_{eff}, H_d, and H_{hf}. Instead, we have in this case

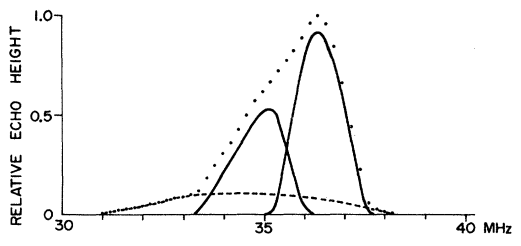

FIG. 4. Reconstruction of the $SmAl_2$ profile with [111] domain assignment.

$$H_{\text{eff}}^2 = H_{\text{hf}}^2 + H_{\text{d}}^2 , \tag{10}$$

and it is no longer possible to determine H_d^{expt} and H_{hf} separately. However, since H_d is much smaller than H_{hf} and since for [100] domain H_d is added only in quadrature to H_{hf}, it makes hardly any difference on derived H_{hf} values whether one uses in (10) H_d^{cal} or some reasonably enhanced value. The H_{hf} results listed in Table I for all of the [100] samples were derived by using $H_{\text{d}}^{\text{enhanced}} = 1.3\, H_d^{\text{cal}}$, where the value of $\alpha = 1.3$ is about the average of the enhancement factors obtained in the [111] compounds $GdAl_2$, $TbAl_2$, and $SmAl_2$ ($HoAl_2$ was not taken into account for reasons given below).

$NdAl_2$. The analysis and the remarks are identical to those of $PrAl_2$.

$DyAl_2$. The analysis and the remarks are identical to those of $PrAl_2$.

$HoAl_2$. From a comparison of the intensities of the two lines at 12.8 MHz and at 25.6 MHz [Fig. 1(g)] and from a comparison of the echo modulation frequencies of the different [111] samples, it must be concluded that [111] domains are preferred in $HoAl_2$, too. Since a lower value of the dipolar field H_d^{expt} is derived than expected from free-ion arguments, α cannot be interpreted in a definite way. Both anisotropic exchange interaction and deviation from free-ion moment may be the reason for the observed behavior.[23] Therefore, $HoAl_2$ was not used to derive the average enhancement α.

For comparison, Table I includes also values of H_d and H_{hf} which would result from the improbable interpretation of the $HoAl_2$ signals as [110] domain lines.

A concise summary of the properties derived or calculated in the present section, such as experimental easy direction of magnetization, $\vec{H}_d^{\text{cal}}$, $\vec{H}_d^{\text{expt}}$, α, and $\vec{H}_{\text{hf}}$ is given in Table I.

IV. MODEL CALCULATION OF MAGNETIC ANISOTROPY

Ignoring shape anisotropy, the magnetic anisotropy energy in crystals with localized magnetic moments arises from the interplay of three major interactions, and the relevant Hamiltonian $\mathcal{H}_m$ is written

$$\mathcal{H}_m = \mathcal{H}_{\text{dip}} + \mathcal{H}_{\text{cf}} + \mathcal{H}_{\text{ex}} , \tag{11}$$

where $\mathcal{H}_{\text{dip}}$ represents the magnetic dipole-dipole interaction between the localized moments, $\mathcal{H}_{\text{cf}}$ is the crystal field Hamiltonian representing the interaction of the electron shells with the crystalline environment, and $\mathcal{H}_{\text{ex}}$ represents the spin-spin exchange interaction between the localized spins. In the case of the RAl_2 system (except for $GdAl_2$ which is excluded from the present treatment) all three mechanisms lend themselves to a convenient theoretical treatment. $\mathcal{H}_{\text{dip}}$ is the easiest to deal with: It simply vanishes in the RAl_2 because of the cubic point symmetry of the R sites (see Sec. III). This can also be verified by performing a summation similar to that of Eq. (4), but with $\vec{r}_i$ being now the vector distance from R_i sites to a given R site. $\mathcal{H}_{\text{cf}}$ is well known theoretically, and apart from a constant, it can be written explicitly for the various R^{3+} multiplets in the required cubic symmetry. A question might exist as to the proper form of $\mathcal{H}_{\text{ex}}$. The R_i-R_j exchange interaction which is usually expressed in terms of an effective exchange constant J_{eff} defined by

$$\mathcal{H}_{\text{ex}} = -2J_{\text{eff}}\vec{S}_i \cdot \vec{S}_j \tag{12}$$

is in fact an indirect interaction[5] arising through the Γ_{sf} coupling between the f shells and the conduction band. Strictly speaking, Eq. (12) is valid only for isotropic Γ_{sf}. As shown in the present study (Secs. III and V) there is evidence for ~ 5% anisotropy in the s-f exchange polarization and therefore some anisotropy is to be expected also for J_{eff}. As will be shown below in the present section, the observed [111] domains in $HoAl_2$ (and perhaps also the [111] domains of $GdAl_2$) are indeed indicative of the importance of the anisotropic exchange interaction. However, the lowest-order term (i.e., the dipolar term) of such anisotropy does not contribute to $\mathcal{H}_{\text{ex}}$ for the same reason that causes $\mathcal{H}_{\text{dip}}$ to vanish, and we shall first assume therefore that (12) is a good approximation to $\mathcal{H}_{\text{ex}}$. The explicit Hamiltonian used for the calculation is thus written

$$\mathcal{H} = \mathcal{H}_{\text{cf}} + \mathcal{H}_{\text{ex}} = \sum_{K,q} A_K^q \langle r^K \rangle Y_K^q(\theta, \phi) + 2\vec{S} \cdot \vec{H}_e , \tag{13}$$

where $Y_K^q(\theta, \phi)$ is the spherical harmonic of degree K and azimuthal quantum number q, $\langle r^K \rangle$ is the mean value of the Kth power of the $4f$-electron radius, and the A_K^q's are parameters related to the strength of the crystal field. $\vec{S}$ is the spin vector of the rare-earth ion and $\vec{H}_e$ is the exchange field acting on it.

In addition to the ground-state level, we have taken into acount in $\mathcal{H}_{\text{cf}}$ the influence of the first excited electronic level, and in Sm, both the first and the second excited electronic levels. Therefore we did not use Stevens's equivalent operator technique[24] in obtaining the matrix elements of the crystal term, but rather employed the method shown by Elliot, Judd, and Runciman[25] using operator techniques developed by Racah. A detailed description of the method, followed by tabulation of the relevant reduced matrix elements, is given by Weber and Bierig.[26] The matrix elements of the term $2\vec{S} \cdot \vec{H}_e$ are the same as those of $2(g_J - 1)\vec{J} \cdot \vec{H}_e$ within a J manifold, and are given by Elliot and Stevens[27] for elements between states not belong-

TABLE IV. Calculated $\vec{M}$ direction for minimal free energy in ferromagnetic RAl_2.

$PrAl_2$	$NdAl_2$	$SmAl_2$	$TbAl_2$	$DyAl_2$	$HoAl_2$	$ErAl_2$
[100]	[100]	[111]	[111]	[100]	[100]	[111]

ing to the same J manifold.

As the point symmetry of the rare-earth ion sites in the RAl_2 system is cubic, the only non-vanishing terms in the crystal field Hamiltonian are those with K equal to 4 or 6 and q equal to 0 or 4. Furthermore, the ratios A_4^4/A_4^0 and A_6^4/A_6^0 are fixed so we are left with two parameters, A_4 and A_6.

As a function of these two parameters, and taking as H_e the exchange fields obtained from the Curie temperatures of the various RAl_2 compounds using the molecular field approximation, the Hamiltonian was constructed, diagonalized to obtain eigenvalues E_i in each compound, and the free energy of the rare-earth ion at temperature T was calculated by

$$F = -kT \ln Z \ , \tag{14}$$

where Z is the partition function given by

$$Z = \sum_i e^{-E_i/kT} \ , \tag{15}$$

the summation being on all the sublevels participating in the Hamiltonian. The whole procedure was carried out for the three major cubic symmetry directions, ⟨100⟩, ⟨111⟩, and ⟨110⟩, and for $T = 4.2\,^{\circ}\mathrm{K}$. The easy direction of magnetization, which still depends on the size of $A_{4,6}$, would be the one possessing the minimal free energy.

Selecting A_4 and A_6 values to fit any *one* of the experimentally determined easy directions, except for $HoAl_2$, the theoretically predicted easy directions of *all* the systems are listed in Table IV. A comparison of Table IV with the experimental observations, with the exception of $HoAl_2$, (Table I, line 1) is self-explanatory. It is found that to obtain correct predictions, A_4 must be positive, and one cannot set limits to its magnitude. There is no evidence for A_6 not being zero, but if $A_6 \neq 0$, then $A_6 < 0$ and no limit can be set on $|A_6/A_4|$.

It is reassuring to note that the above predictions are also in agreement with experimental determination of A_4 and A_6 reported recently for $CeAl_2$ [Ref. 2(b)] and $ErAl_2$.[2(c)] However, there is at least one compound for which the simple Hamiltonian (13) seems to be inadequate. For $A_4 > 0$ and $A_6 \leq 0$ as determined above, the model prediction for $HoAl_2$ is ⟨100⟩ easy direction if $|A_6/A_4| \leq 0.045\ r_0^{-2}$, and ⟨110⟩ easy direction if $|A_6/A_4| > 0.045\ r_0^{-2}$, neither of which is in accord with the results of Sec. III (r_0 is the Bohr radius). If, on the other hand, $A_{4,6}$ are adjusted to obtain agreement with the ⟨111⟩ observation, it is found that $A_4 < 0$, $A_6 \geq 0$ are required, i.e., one will have to make the unlikely assertion that the crystal field parameters of $HoAl_2$ have opposite signs to those of all the other RAl_2 on which data is available. In view of the above discrepancies, it is reasonable to conclude that anisotropic exchange terms, not included in the simple Hamiltonian (14), are not negligible in at least some of the RAl_2 compounds.

V. *s-f* EXCHANGE INTERACTION

As stated earlier, the conventional relation between H_{hf} and Γ_{sf} [Eqs. (2) and (3)] would hold only when assuming that the conduction electrons form a parabolic band. In fact, it has been demonstrated theoretically[17(c)] that even for a spherical conduction band, a relation like (3) holds only for S-state localized moments and anisotropy in Γ_{sf} is expected for non-S R ions. We shall return to the anisotropy problem below, but even granting the validity of (3), it is clear that the Γ_{sf} can be determined experimentally only up to a constant factor. Thus, assuming that $A^{27}(0)$ and E_f are constants, a "reduced" exchange parameter can be derived from H_{hf} values by writing

$$\Gamma_{sf}^{\mathrm{red}} = \frac{\Gamma_{sf}}{\Gamma_{sf}(GdAl_2)} = \frac{H_{\mathrm{hf}}/(g_J - 1)J}{H_{\mathrm{hf}}(GdAl_2)/\frac{7}{2}} \ . \tag{16}$$

Variation of E_f is not impossible (e.g., in the parabolic-band approximation with constant m^*, the 2.5% contraction of a as we move from $PrAl_2$ to $HoAl_2$ would result in a 5% overall increase of E_f across the system), but will be ignored in the present discussion. $\Gamma_{sf}^{\mathrm{red}}$ values are listed at the bottom of Table I, and it is seen that the full accuracy of the experimental measurements is retained for the purpose of comparisons within the series.

We return now to the problem of anisotropic Γ_{sf} which was mentioned at the beginning of this section. To date, there has been no experimental evidence for such anisotropy and we believe that the significant deviation of H_d^{expt} from H_d^{cal} that was observed in two out of the four ⟨111⟩ compounds for which the comparison could be made provides direct evidence for the existence of anisotropic localized-spin conduction-electron exchange interaction in a metallic rare-earth system. The degree of anisotropy for each compound can be expressed numerically by the ratio between the maximum and minimum exchange polarizations observed at different $\vec{M}$ directions. Within the framework of the phenomenological model which was utilized in the analysis (Sec. III), the anisotropic s-f exchange term is expressed in a dipolar form and with the help of Eqs. (3) and (4) we finally obtain

$$A_n = \frac{\Gamma_{sf}(\max)}{\Gamma_{sf}(\min)} - 1$$

$$= \frac{H_{\rm hf} + (\alpha - 1)H_d^{\rm cal}(\vec{M}\|[111], a \text{ site})}{H_{\rm hf} - (\alpha - 1)H_d^{\rm cal}(\vec{M}\|[110], \text{sites } b_1 \text{ or } b_2)} - 1 .$$

Using α values from Table I and $H_d^{\rm cal}$ values from Table III, it is found

$$A_n(GdAl_2) = 0.031 \pm 0.008,$$

$$A_n(TbAl_2) = 0.17 \pm 0.04 .$$

From the present data it is not possible to determine with certainty the origin of the anisotropy, but a comparison of A_n in $GdAl_2$ to that of $TbAl_2$ supports a speculation that only a small part of the anisotropy may be attributed to the conduction band being aspherical (i.e., in $GdAl_2$), whereas most of the anisotropy is caused by nonspherical localized f shells (such as exist in $TbAl_2$). The second mechanism has been treated to some extent in the WKPF theory,[17(c)] but the effect of nonspherical conduction band on Γ_{sf} has not been treated, as yet, in quantitative manner applicable to the present system.

For a complete discussion of the behavior of Γ_{sf} across the series, it would have been desirable to have at least Γ_{sf} *and* A_n values for all of the compounds. Unfortunately, as things stand now only the isotropic part of Γ_{sf}, as represented by $\Gamma_{sf}^{\rm red}$ in Table I, is available over a reasonable range in the system. Moreover, these Γ_{sf} reflect mostly variation of $J_{\rm eff}(2k_F)$,[17(d)] whereas WKPF treats the variation across the series only for diagonal part $J_{\rm eff}(0)$ of the exchange. It has been demonstrated theoretically that in general $J(0) \neq J(2k_F)$,[17(e)] and it is not clear that one can prove proportionality between the two all across the series. Anyhow, hoping that some scaling does exist and assuming that the anisotropic part of the exchange tends to average out during the integration over $\vec{K}$ in the WKPF theory, a comparison is presented in Fig. 5 where the experimental Γ_{sf} and theoretical $J_{\rm eff}(0)$ are displayed together in reduced scale units related to $GdAl_2$. The theoretical curve has been "best fitted" to the data by selecting $k_F \simeq 1.1$ a.u. (to be compared with the free-electron value, $k_F \simeq 0.86$ a.u., in the RAl_2 system) and $\Delta E_{ab} = \Delta E_{em} \simeq 2$ eV,[28] but in view of the remarks above and because of the general nature of the WKPF theory, one should not attach too much significance to the actual values of the adjusted parameters. The last point is manifested by the fact that while there is a general agreement between theory and experiment, there are still deviations notably for $NdAl_2$ and $HoAl_2$ which are at present larger than the experimental probable error. Also plotted in Fig. 5 are "reduced"

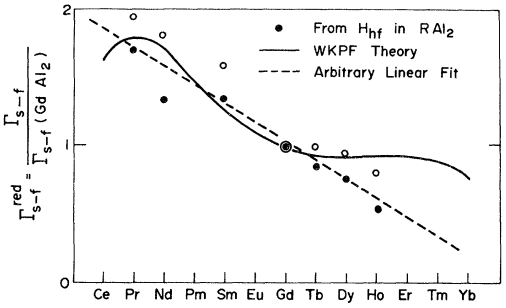

FIG. 5. Experimental and theoretical variation of $\Gamma_{sf}^{\rm red}$ across the RAl_2 system (see text for details). Open circles represent "reduced" Γ values derived from T_c.

Γ values derived from T_c by the de Gennes relation.[5(b)] As mentioned in the introduction, however, $\Gamma(T_c)$ may reflect also direct exchange mechanisms which are not discussed in the present study. We believe that Fig. 5 would have served its purpose even if its sole effect is to inspire a theorist to develop a detailed exchange theory tailored specifically to the RAl_2 system.

VI. CONCLUDING REMARKS

We have been able to derive from the ^{27}Al nmr absorption in ferromagnetic RAl_2 (a) easy directions of magnetization and (b) anisotropic and isotropic s-f exchange parameters.

A simple model calculation of the magnetic energy has been developed and the model predictions are in agreement with the observation throughout the system, except for $HoAl_2$. It should be remembered, however, that in developing the model, it was assumed throughout that the effective R-R exchange in all the compounds is isotropic. The existence of higher-order anisotropy terms in the exchange Hamiltonian may lead to other patterns of magnetic anisotropy energy which are not predicted by the present simple model. That such anisotropy can exist is evident from the experimentally observed s-f anisotropy. The small (< 5%) helical antiferromagnetism that had been observed by neutron diffraction to be superimposed on the ferromagnetic order in $DyAl_2$ (Ref. 3) and the behavior of $HoAl_2$ as described in the present study might be the manifestation of such anisotropic R-R exchange. Because of inhomogeneous broadening of the NMR lines in powder samples (Sec. III) the present technique may not be used to detect small deviations of $\vec{M}$, and small superstructures like that of $DyAl_2$,[3] even if they exist in some of the RAl_2 that have been studied, will remain unnoticed.

Concerning the s-f exchange, we have demonstrated the existence of ~ 10% anisotropy in Γ_{sf}. A systematic experimental study of the phenom-

enon is not possible with powder samples under zero external field because many of the compounds order spontaneously in the ⟨100⟩ direction, in which case the anisotropy cannot be observed because of symmetry consideration (Sec. III). The difficulty may be removed in principle by studying the NMR profiles in uniformly magnetized single-crystal samples where $\vec{M}$ can be directed at will by an external magnetic field. In practice, however, the experimental difficulties involved in a single crystal study are not very simple to overcome.

The behavior of the isotropic part of Γ_{sf} seems to follow the general theory—or perhaps it is the other way around—but the relative accuracy of the experimental data has yet to be matched by an equally accurate theoretical treatment.

ACKNOWLEDGMENTS

Stimulating discussions with H. J. van Daal, R. E. Bauminger, and B. Elschner and experimental contributions of A. Oppelt are gratefully acknowledged. One of us (N. K.) acknowledges with thanks the warm hospitality accorded him by the people of the II Physikalisches Institut during his stay at the T. H. Darmstadt. The work performed at the T. H. Darmstadt is affiliated with the "S. F. B. Festkörperspektroskopie Darmstadt/Frankfurt."

---

*Permanent address: The Racah Institute of Physics, The Hebrew University, Jerusalem.

[1]J. H. Wernick and S. Geller, Trans. AIME 218, 958 (1960).

[2](a) H. J. Williams, J. H. Wernick, E. A. Nesbitt, and R. C. Sherwood, J. Phys. Soc. Japan 17, suppl. B-I, 91 (1962); (b) R. W. Hill and J. M. Machado da Silva, Phys. Letters 30A, 13 (1969); (c) H. G. Purwins, Z. Physik 233, 27 (1970).

[3]N. Nereson, C. Olsen, and G. Arnold, J. Appl. Phys. 37, 4575 (1966).

[4]N. Nereson, C. Olsen, and G. Arnold, J. Appl. Phys. 39, 4605 (1968).

[5](a) K. Yosida, Phys. Rev. 106, 893 (1957); (b) P. G. de Gennes, J. Phys. Radium 23, 510 (1962).

[6]V. Jaccarino, B. T. Matthias, M. Peter, H. Suhl, and J. H. Wernick, Phys. Rev. Letters 5, 251 (1960).

[7]V. Jaccarino, J. Appl. Phys. 32, 102S (1961).

[8]S. Koide and M. Peter, Rev. Mod. Phys. 36, 160 (1964).

[9]E. D. Jones and J. I. Budnick, J. Appl. Phys. 37, 1250 (1966).

[10](a) R. G. Barnes and E. D. Jones, Solid State Commun. 5, 285 (1967); (b) W. H. Jones, Jr., T. P. Graham, and R. G. Barnes, Phys. Rev. 132, 1898 (1963); (c) K. H. J. Buschow, A. M. van Diepen, and H. W. de Wijn, Phys. Letters 24A, 536 (1967).

[11]K. H. J. Buschow, J. F. Fast, A. M. van Diepen, and H. W. de Wijn, Phys. Status Solidi 24, 715 (1967).

[12]H. J. van Daal and K. H. J. Buschow, Solid State Commun. 7, 217 (1969).

[13]F. Dintelmann, E. Dormann, and K. H. J. Buschow, Solid State Commun. 8, 1911 (1970).

[14](a) N. Shamir, N. Kaplan, and J. H. Wernick, J. Phys. Paris 32, C1-902 (1971); (b) R. E. Gegenwarth, Ph. D. thesis (Fordham University, 1967) (unpublished).

[15]F. Dintelmann and K. H. J. Buschow, Z. Angew. Phys. 31, 181 (1971).

[16]E. Dormann, K. H. J. Buschow, and K. N. R. Taylor, J. Phys. F (to be published).

[17](a) A. J. Freeman and R. E. Watson, Phys. Rev. 127, 2058 (1962); (b) J. O. Dimmock and A. J. Freeman, Phys. Rev. Letters 13, 750 (1964); (c) R. E. Watson, S. Koide, M. Peter, and A. J. Freeman, Phys. Rev. 139, A167 (1965); (d) See, for example, R. E. Watson, in *Hyperfine Interactions*, edited by A. J. Freeman and R. B. Frankel (Academic, New York 1967), p. 419ff; (e) R. E. Watson and A. J. Freeman, Phys. Rev. 152, 566 (1966).

[18]Naokatsu Sano, Shun-ichi Kobayashi, and Junkichi Itoh, Progr. Theoret. Phys. (Kyoto) Suppl. 46, 84 (1970).

[19]No errors are quoted in Ref. 10(a), but in view of the errors quoted in Ref. 6 and the discussion of Ref. 10(b), an error limit of ±30% is not unlikely for derivation from Knight shifts.

[20]Additional broadening exists because of ^{27}Al quadrupole interaction [see Refs. 6 and 14(a)]. The effect would be somewhat smaller than the effect of demagnetization except for very small $\vec{M}$.

[21]This procedure was followed in the preliminary analysis described in Ref. 14(a).

[22]Another correction may enter into H_d^{expt} because of the spatial spin distribution over the entire f shell. We have calculated this correction numerically, utilizing Gd $4f$ wave functions from Ref. 17(a), and found it to be negligible for the RAl_2 system in the present context.

[23]In actual fact, using H_d^{cal} as a reference tends to underestimate the size of the anisotropic s-f exchange contribution in the present context. As is well known, there are systems in which the experimentally determined localized R moments are smaller than the free-ion value used in deriving H_d^{cal} (see Refs. 2–4). One may even anticipate negative value of $H_d^{\text{expt}} - H_d^{\text{cal}}$ for systems where the local moments are substantially smaller than $g\mu_B\vec{J}$.

[24]K. W. H. Stevens, Proc. Phys. Soc. (London) A65, 209 (1952).

[25]J. P. Elliot, B. R. Judd, and W. A. Runciman, Proc. Roy. Soc. (London), A240, 509 (1957).

[26]M. J. Weber and R. W. Bierig, Phys. Rev. 134, A1492 (1964).

[27]R. J. Elliot and K. W. H. Stevens, Proc. Roy. Soc. (London) A218, 553 (1953).

[28]See Ref. 17(c) for details. Very crudely, $\Delta E_{a,e}$ can be visualized as the splitting of the virtual levels of a localized $4f$-type electron or hole above or below E_F, respectively.